

Demonstration of an Error-Free 4×10 Gb/s Multiuser SPECTS O-CDMA Network Testbed

Ryan P. Scott, Wei Cong, Kebin Li, Vincent J. Hernandez, Brian H. Kolner, *Senior Member, IEEE*, Jonathan P. Heritage, *Fellow, IEEE*, and S. J. Ben Yoo, *Senior Member, IEEE*

Abstract—We demonstrate an error-free four-user 10-Gb/s/user optical code-division multiple-access network testbed employing the spectral phase encoded time spreading technique and nonlinear thresholding. The experiments successfully overcome multiuser interference, resulting in error-free operation.

Index Terms—Multiaccess communication, nonlinear detection, optical code-division multiple-access (O-CDMA), optical fiber communications.

I. INTRODUCTION

RECENT advances in wavelength-division-multiplexing (WDM) and time-division-multiplexing (TDM) technologies have fueled rapid deployments of optical networking in metro- and wide-area networks. Local-area networks (LANs), on the other hand, have requirements that are not easily met by WDM or TDM technologies. Additional hardware and protocols imposed by WDM and TDM at the distributing nodes unfavorably add to the cost and complexity of the LAN. Optical code-division multiple-access (O-CDMA) allows very flexible access to the large communication bandwidth available in optical networks and a capability of concealing data content. This is possible without relying on complex distribution nodes but with simple reconfiguration of codes at end-user nodes. Many implementations of O-CDMA, using a variety of coding and detection schemes, have been investigated in the last 15 years [1]–[4]. The key challenge in realizing scalable and viable O-CDMA networks lies in overcoming interference from many simultaneous users [multiple-user interference (MUI)].

This letter discusses a synchronous O-CDMA system based on a spectral phase-encoded time-spreading (SPECTS) technique which encodes or decodes by individually phase-shifting slices of optical spectrum (chips) [5]. Each encoder or decoder consists of a fiber pigtailed zero-dispersion pulse shaper [5] that spatially decomposes a short optical pulse into the spectral domain and a liquid crystal spatial light modulator (LC-SLM) that phase modulates the spectrum (0 or π radians/chip). All

users are encoded with 64-chip Walsh codes in this synchronous system and operate at OC-192 (9.953 28 Gb/s) data rates, allowing us to realistically evaluate the impact of MUI. Correct decoding takes place when the conjugate of a user's Walsh code is applied at the receiver in another pulse shaper and the original pulse is reconstructed. Since the reconstructed pulses are much shorter than the receiver's impulse response, a nonlinear thresholder is then necessary to differentiate between correctly and incorrectly decoded pulses. We employ a thresholder based on highly nonlinear fiber (HNLf) and a fiber-based longpass filter which proved strikingly effective in the presence of MUI. The HNLf increased our thresholder's sensitivity by more than five-fold when compared to the dispersion-shifted fiber-based thresholder described in [6]. Recent work from our group has demonstrated a single-user SPECTS O-CDMA system at high bit rates [7] and, here, we present an error-free four-user 10-Gb/s O-CDMA testbed, we believe, for the first time.

II. EXPERIMENTAL SETUP

Fig. 1 is a diagram of the four-user SPECTS O-CDMA testbed that allows truly uncorrelated worst-case multiuser experiments. A 10-Gb/s mode-locked fiber laser centered at 1550 nm produces 2.5-ps pulses which are amplified and compressed to approximately 0.5 ps by a nonlinear fiber-based compressor. A pseudorandom pattern generator drives an intensity modulator and impresses $2^{31} - 1$ pseudorandom binary sequence data onto the compressor output. The modulated pulse stream is split into four separate streams after amplification by a dispersion-compensated Erbium-doped fiber amplifier (DC-EDFA). To simulate four independent users, Outputs 2–4 of the 1:4 coupler are time delayed 40, 80, and 128 bits and pulse-aligned (± 1 ps) with Output 1 using variable time delays.

The SPECTS encoders apply a different 64-chip Walsh code to each user signal and in this experiment, User 1 is correctly decoded (the intended user), while Users 2–4 are incorrectly decoded (the interfering users). In synchronous systems, Walsh codes exhibit superior MUI suppression compared to other known codes due to their characteristic intensity minimum at temporal center. Users 1–4 utilized the 5th, 54th, 52nd, and 32nd codes from the Walsh 64 code set, respectively. Individual user signal powers are equalized by variable attenuators and recombined in a 4:1 coupler. A DC-EDFA corrects for system losses and the combined users' signals pass through the SPECTS decoder that applies the intended user's conjugate Walsh code. Careful cross-correlation measurements taken on each of the four encoders revealed the time spread pulses closely resemble those theoretically predicted from

Manuscript received March 16, 2004; revised June 2, 2004. This work was supported in part by DARPA and SPAWAR under agreement N66001-02-1-8937 and in part by the AFOSR through the UC Davis Center for Digital Security.

R. P. Scott, W. Cong, and B. H. Kolner are with the Department of Applied Science, University of California, Davis, Davis, CA 95616 USA (e-mail: scott@leorg.ucdavis.edu; wcong@ucdavis.edu; bhkolner@ucdavis.edu).

K. Li, V. J. Hernandez, J. P. Heritage, and S. J. B. Yoo are with the Department of Electrical and Computer Engineering, University of California, Davis, Davis, CA 95616 USA (e-mail: vjhernandez@ucdavis.edu; heritage@ece.ucdavis.edu; sbyoo@ucdavis.edu).

Digital Object Identifier 10.1109/LPT.2004.833038

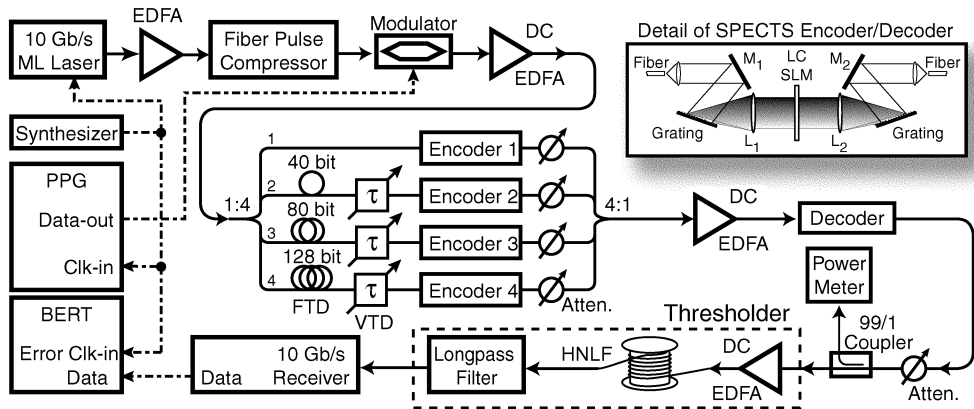


Fig. 1. Diagram of the four user SPECTS O-CDMA setup. Inset shows a schematic of a pulse shaper used for encoders and the decoder. FTD: fixed time delay. VTD: variable time delay. L_1 , L_2 : lenses. PPG: pseudorandom pattern generator. BERT: BER test set.

corresponding Walsh-code simulations. Therefore, in principle, without loss of generality, we chose one of the encoders to be the “intended user” matching the code of the decoder, and the other three encoders to be the “interferers” using different Walsh codes. The encoders and decoder spectrally filter the pulse to a full width of 14 nm (1% of maximum points) and broaden a correctly decoded pulse to 0.8 ps from the 0.5-ps input pulsewidth. Note, most of the spectral filtering that occurs in the pulse shapers is due to wavelength-dependent loss when coupling back into fiber. The spectral resolution of Encoder 1 and the decoder was 0.1 nm and Encoders 2–3 had a spectral resolution of 0.13 nm. The typical fiber-to-fiber insertion loss for the encoders and decoder was 11–13 dB. The attenuator and 1% coupler following the decoder are used to adjust and monitor the threshold input power when making bit-error-rate (BER) measurements. The threshold then suppresses the interferers’ signals and passes the intended user’s signal to an optoelectronic receiver that is electrically filtered by an OC-192 lowpass filter before detection by the BER test set. While the presented network concept and threshold detection scheme are polarization-independent, the gratings and the LC-SLMs in the experiment are polarization-dependent, which required us to use polarization controllers, polarizers, and polarization-maintaining fibers in the experiment.

III. RESULTS AND DISCUSSION

The nonlinear thresholder utilizes 500 m of HNLF (Sumitomo, HNLF 1322AA-2) and a simple C/L -band splitter acts as a longpass filter. The HNLF specifications include a zero-dispersion wavelength of 1543 nm, 0.19-ps/nm/km dispersion at 1550 nm, dispersion slope of 0.026 ps/nm²/km at 1550 nm, effective area of 10 μm^2 , and a nonlinear coefficient of $20 (\text{W} \cdot \text{km})^{-1}$. Fig. 2 shows the transmission characteristics of the longpass filter overlaid with the spectra generated by the intended user plus three interfering users and just the three interferers alone. The high peak power of the user’s signal (Fig. 3) in the HNLF shifts spectral power into longer and shorter wavelengths due to self-phase modulation and other fiber nonlinearities. The longer wavelengths are passed to the receiver through the longpass filter. At the receiver, we measured a power contrast ratio of 23 dB between the intended

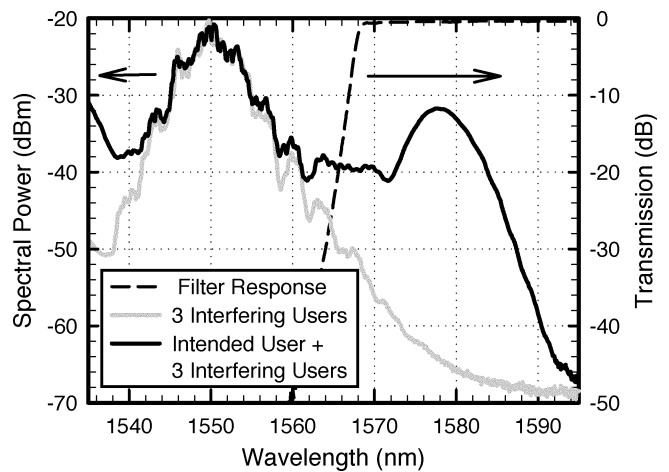


Fig. 2. Spectral plot demonstrating how the thresholder discriminates between the intended user and interfering users’ signals. The high peak power of the intended user’s pulses generate additional spectrum (black trace) when compared to the spectrum from interfering users (gray trace). Spectra greater than 1568 nm are selected by the longpass filter (dashed trace).

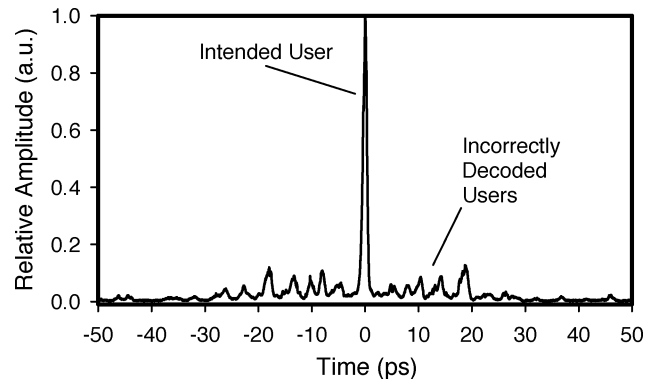


Fig. 3. Cross correlation showing the intended user and three interfering users at the threshold input. The reference pulsewidth is < 400 fs.

user and all three interferers. In Fig. 2, this is essentially the ratio of the integrated spectral power of each trace within the passband of the filter.

Fig. 4(a) presents the BER performance of this multiuser system. The arrows at the bottom of each BER curve indicate the minimum power at which the system operated error-free while collecting more than 3×10^{12} data bits (i.e., the BER was

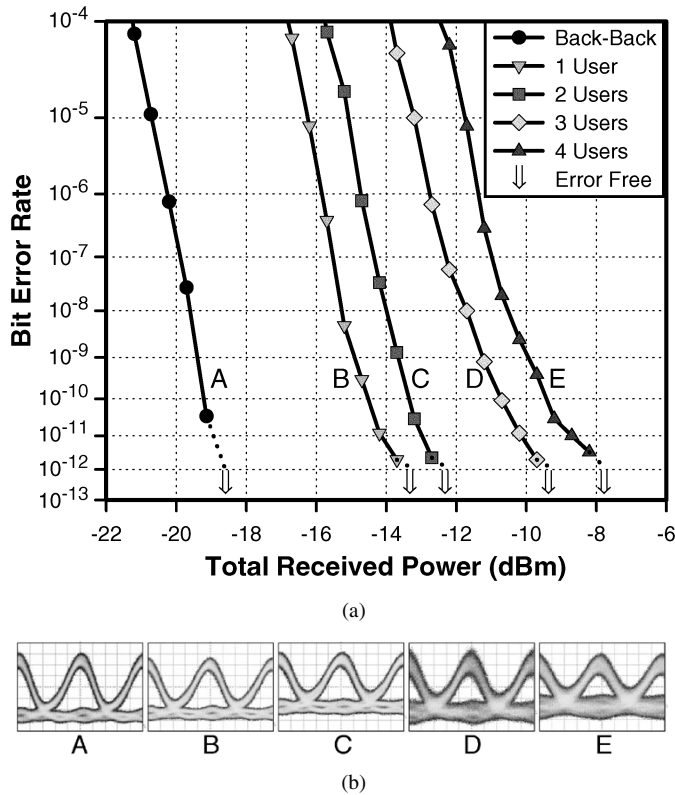


Fig. 4. (a) Plot of BER statistics showing the change in system performance with an increasing number of users. Total received power is the threshold input power and the indicated error-free point is the minimum power at which the BER $< 10^{-12}$. (b) Corresponding eye diagrams for each BER trace.

less than 10^{-12}). Fig. 4(b) presents an eye diagram for each BER curve where the time span of each eye diagram is 200 ps (20 ps/div). The total received power is the measured power at the input of the threshold (see Fig. 1, dashed box). The back-to-back BER data (Trace A) are taken with just a single user; sans encoders, decoder, and intervening DC-EDFA. The other BER data are for the intended user alone (Trace B), and then the intended user with an additional one to three interfering users (Traces C–E, respectively). The average output power of the threshold DC-EDFA was set to 14 dBm for Traces A and B and the power penalty arises from pulse broadening, presumably due to the spectral filtering and residual dispersion in the encoder and decoder. As each interfering user was added, the average output power of the threshold DC-EDFA was increased to keep the intended user's average power into the HNLFF constant (i.e., threshold DC-EDFA output of 17, 18.8, and 20 dBm for Traces C, D, and E, respectively). This measurement arrangement emulates adaptive threshold detection consisting of a DC-EDFA, a HNLFF, and a longpass filter, where the DC-EDFA adjusts its pump power level to

optimize the threshold detection of the intended user's signal while suppressing the interfering signal. Each interfering user contributes a different amount of system penalty due to the differing MUI from unique Walsh codes.

As stated above, the average power of the intended user's signal into the HNLFF was maintained at 14 dBm. This translates to a detection energy of 5 pJ per 800-fs pulse compared to the low detection energy of 0.4 pJ per 400-fs pulse reported in [4]. Despite the 12.5 times higher detection energy requirement (6.3 times peak pulse power), the HNLFF detection scheme used here is polarization-independent and can be used for detection in unpolarized fiber-based O-CDMA networks.

IV. CONCLUSION

We have demonstrated the first error-free SPECTS O-CDMA network testbed with four simultaneous users, each operating at 10 Gb/s. An HNLFF-based nonlinear thresholder successfully discriminated between intended and all interfering O-CDMA users with a contrast ratio of 23 dB. Finally, the BER measurement of the testbed showed outstanding suppression of the MUI effect for an increasing number of simultaneous users.

ACKNOWLEDGMENT

The authors would like to thank PriTel, Inc. and Sumitomo Electric Industries, Ltd. for their generous loan of equipment.

REFERENCES

- [1] J. A. Salehi, A. M. Weiner, and J. P. Heritage, "Coherent ultrashort light pulse code-division multiple access communication systems," *J. Lightwave Technol.*, vol. 8, pp. 478–491, Mar. 1990.
- [2] H. P. Sardesai, C. C. Chang, and A. M. Weiner, "A femtosecond code-division multiple-access communication system test bed," *J. Lightwave Technol.*, vol. 16, pp. 1953–1964, Nov. 1998.
- [3] H. Tsuda, H. Takenouchi, T. Ishii, K. Okamoto, T. Goh, K. Sato, A. Hirano, T. Kurokawa, and C. Amano, "Spectral encoding and decoding of 10 Gbit/s femtosecond pulses using high resolution arrayed-waveguide grating," *Electron. Lett.*, vol. 35, no. 14, pp. 1186–1188, 1999.
- [4] Z. Jiang, D. Seo, S.-D. Yang, D. E. Leaird, A. M. Weiner, R. V. Roussev, C. Langrock, and M. M. Fejer, "Four user, 2.5 Gb/s, spectrally coded O-CDMA system demonstration using low power nonlinear processing," presented at the Optical Fiber Communications Conf. (OFC 2004), Opt. Soc. America, Washington, DC, 2004, Postdeadline Paper PDP29.
- [5] J. P. Heritage, A. M. Weiner, and R. N. Thurston, "Picosecond pulse shaping by spectral phase and amplitude manipulation," *Opt. Lett.*, vol. 10, no. 12, pp. 609–611, 1985.
- [6] H. P. Sardesai and A. M. Weiner, "Nonlinear fiber-optic receiver for ultrashort pulse code division multiple access communications," *Electron. Lett.*, vol. 33, no. 7, pp. 610–611, 1997.
- [7] K. Li, W. Cong, V. J. Hernandez, R. P. Scott, J. Cao, Y. Du, J. P. Heritage, B. H. Kolner, and S. J. B. Yoo, "10 Gbit/s optical CDMA encoder-decoder BER performance using HNLFF thresholder," presented at the Optical Fiber Communications Conf. (OFC 2004), Opt. Soc. America, Washington, DC, 2004, Paper MF87.